Archives of Civil and Mechanical Engineering (2021) 21:80
https://doi.org/10.1007/s43452-021-00229-z

ORIGINAL ARTICLE

Effect of multi-wall carbon nanotubes on the flexural performance of cement based composites

Jun Huang[1,3] · Denis Rodrigue[2] · Peipei Guo[3]

Received: 12 February 2021 / Revised: 2 April 2021 / Accepted: 16 April 2021 / Published online: 3 May 2021

Abstract

In this work, multi-wall carbon nanotubes (MWCNT) are added (0–0.5 wt%) into a cement matrix to improve the flexural performance of the resulting nanocomposites. Under static testing, the compressive and flexural strengths were found to increase with MWCNT content with an optimum content of 0.2% and 0.1%, respectively, before decreasing because of dispersion problems (agglomeration). But it was observed that increasing the mixing time and adding silica fume improved the MWCNT dispersion. Under fatigue testing, similar trends were obtained with respect to MWCNT content as the maximum fatigue life was observed at 0.2%. A comparison between nano-silica and MWCNT reinforced concrete is also made showing that MWCNT provides better improvement at lower content. The MWCNT reinforced cement-based composite results were well fitted using linear regressions. Finally, a morphological analysis via scanning electron microscopy (SEM) was performed to explain the results based on the micro-mechanical mechanism of MWCNT reinforced composites.

Keywords Multi-wall carbon nanotube · Cement · Strength · Fatigue life · Regression analysis · Morphology

1 Introduction

Concrete is a quasi-brittle material. When cyclic loading is applied on a specimen, it can fracture due to fatigue at a stress level much lower than its ultimate static strength. But several methods were proposed to improve the fatigue performance of concrete such as the addition of different types of fibers or fillers. Despite the conflicting information reported in the literature regarding the fatigue behavior of concrete, several works observed that particle addition can improve the fatigue performance of concrete [1]. Nevertheless, a material can be used under several types of loads such as static (compression, tension, flexion, shear, etc.) and dynamic (impact, fatigue, etc.) loadings. But their combination is also possible (multi-axial).

Compressive fatigue testing is easy to implement and often selected to investigate the mechanical properties and fatigue resistance of concrete [2]. Medeiros et al. presented that the compressive fatigue life of composites at lower frequencies is less than that at higher frequencies, especially for the plain concrete [3]. But compared with compressive tests, reports on tensile fatigue testing of fiber reinforced concrete are very limited because of the difficulty of loading the samples. Nevertheless, De Andrade Silva et al. [4] investigated the fatigue behavior of sisal fiber (10% volume fraction) reinforced cement-based composites under stress levels ranging from 0.3 to 0.8. Makita et al. [5] studied the tensile fatigue behavior of steel fiber (3 vol%) reinforced concrete under stress levels ranging from 0.45 to 0.70. Furthermore, from the tensile fatigue test of plain concrete and steel fiber reinforced concrete, Isojeh et al. [6] reported that the fatigue life of these materials increased with increasing steel fiber volume fraction from 0 to 1.5%.

Although several fatigue loading modes are possible, flexural fatigue loading is the easiest to implement which can also give information on the tensile properties. This is why it is widely adopted to quantify the fatigue performances of cement-based composites. To improve the fatigue performance of concrete, different types of fibers were used alone, such as carbon [7], polypropylene [8], glass [9],

✉ Jun Huang
junhd@wzu.edu.cn

1 College of Civil Engineering and Architecture, Wenzhou University, Wenzhou, China

2 Department of Chemical Engineering, Laval University, Quebec, Canada

3 School of Civil Engineering and Architecture, Guangxi University of Science and Technology, Liuzhou, China

steel [10], and recycled tire polymer (52% PET, 39% PA 66 and 9% PBT) [11], etc. The results obtained from Wang et al. [12] showed that carbon fibers improved the cracking resistance and had a beneficial effect on the fatigue life and energy absorption capacity of concrete. Mohamadi et al. [13] reported that polypropylene fibers can increase resistance against fatigue crack growth under both constant and variable amplitude loading. Due to their lower price and higher tensile strength (over 1 GPa), steel fibers are widely used to improve the fatigue properties of concrete. With small sized specimens, Carlesso et al. [14] proved that steel microfiber will be pull-out rather than a fatigue failure when the fatigue failure of high performance concrete occurs. For the large scale steel fiber reinforced concrete beams, the results [15] showed an increased fatigue life of 47 and 182% when the steel fiber volume fraction was taken as 0.4 and 0.8%. Furthermore, Saoudi and Bezzazi [16] studied the effects of strait (smooth) and hook-end steel fibers on the fatigue performance of concrete. The result showed that steel fibers can increase the bending strength and decrease the deflection of concrete. Graeff et al. [17] selected recycled steel fibers to substitute the industrially produced steel fibers and analyzed their role on improving the fatigue behavior of concrete. It was shown that 2% wt of recycled steel fiber gave the best fatigue performance. Smrkić et al. [18] also reported that recycled steel fibers can be used as an alternative to standard steel fibers to reinforce concrete based on engineering, economic and ecological aspects. Using a blend of manufactured and recycled tire steel fibers, the fatigue stress resistance of concrete was improved by 11% compared to the plain concrete [19]. In addition, Al-Azzawi et al. [20] reported that a uniform fiber distribution can lead to a very high fatigue endurance limit when brass-coated steel fibers were added into the matrix. Compared with the normally vibrated steel fiber reinforced concrete, self-compacting concrete is more attractive [21]. It was shown that adding steel fibers into self-compacting concrete led to higher fatigue strength (two-million cycles) from 62% of the corresponding static strength to 71% compared with the normally vibrated fiber reinforced concrete when steel fiber volume fraction is 1.5% [22]. On the basis of the previous three-point bending fatigue tests, Goel et al. [23] further investigated the fatigue performance of four-point bending beams, similar results were gotten. From a fracture mechanics point of view, Germano et al. [24] investigated the fatigue behavior of steel fiber (0.5 and 1.0 vol%) reinforced concrete notched beams. The results showed that the fatigue performance was increased as higher energy dissipation was generated up to failure. Then, the effect of cyclic loading magnitude on the fatigue fracture of composites was further studied for notched concrete beams [25]. In particular, mineral particles addition (fly ash, silica fume, etc.) was investigated by Kaur et al. [26] to compare the fatigue life curves of steel fiber reinforced concrete leading to different failure probabilities. Rios et al. [27] also presented a probabilistic model to explain the relation between the fatigue behavior and steel fibers distribution in reinforced concrete for continuous damage under flexion. They proposed a model including a scale parameter, shape parameter and location parameter. With numerical simulation methods, Banjara and Ramanjaneyulu [28] were able to predict the fatigue life of steel fiber reinforced concrete based on a fracture mechanics approach and the results were well correlated with the experimental data.

Mulheron et al. [29] compared the effect of different fibers, such as polypropylene, steel or carbon, on the fatigue strength and toughness of concrete. Based on the Weibull function, Huang et al. [30] proposed a new model to predict the fatigue life of fiber reinforced concrete, in which the fiber type and fiber content were included in the model parameters.

Finally, instead of using a single fiber reinforcement, the possibility to combine different fibers together can lead to synergistic effect by the production of hybrid composites. This option was shown to generate several advantages like improved fatigue behavior of concrete [31].

Although several reports on the effect of macro fibers on the fatigue performance of concrete are available, the information on the fatigue behavior of nano-particle reinforced concrete is very limited. Today, carbon nanotubes (CNT) have one of the highest elastic modulus (1 TPa) and tensile strength (over 25 GPa), and a low content (1–2%) can have a significant effect on the mechanical properties of the resulting nano-composites. Sobolkina et al. [32] investigated the effect of CNT content (0.05–0.25%) on the compressive strength of cement paste. The results showed that the well dispersed CNT (mixed and nitrogen doped CNT) led to significant increases (35% and 12%) in compressive strength under dynamic loading. Kumar et al. [33] used three CNT weight fractions (0.5%, 0.75% and 1.0%) and determined that the optimal CNT content was 0.5% with 15% increase in compressive strength. From a micro-structure point of view, fly ash can also be added into a cement matrix leading to a further compressive strength increase (8%) of the cement-based composites with 0.5% CNT [34]. Kim et al. [35] showed that adding silica fume (10%, 20% or 30%) can lead to less CNT agglomeration resulting in higher compressive strength. Furthermore, CNT coated with a solid nano-silica shell was added into the matrix and the compressive strength increased by 19% and 20% at 0.125% and 0.25% CNT, respectively [36]. To improve flexural strength, CNT can be used to increase the interfacial adhesion between the reinforcement and concrete leading to better flexural loading capacity (24% higher) of the composites [37]. Rocha et al. [38] also reported that the flexural strength of cement composites can be increased by 46% with the addition of only 0.1% wt CNT.

From the literature available, several papers focused on the effect of CNT content on the static mechanical properties of cement-based composites. However, the fracture of cementitious composites is mainly resulting from long term loadings. Furthermore, when the composites are subjected to cyclic loading, the specimen will break under a load which can be substantially lower than its ultimate strength. For this reason, this study systematically investigates the flexural properties of MWCNT reinforced cement-based composites under static loading and cyclic loading. The effect of silica fume and fly ash addition is also considered.

2 Experimental preparation

2.1 Materials

In this study, multi-wall carbon nanotube (MWCNT) dispersions were obtained from Beijing BOYU GAOKE new material co. Ltd. (China). The compounds are composed of MWCNT, dispersant and deionized water. The mass fraction of MWCNT in the dispersion is 10% and was obtained via ultrasonic crusher and centrifugal sedimentation. The MWCNT purity is above 98% and the length ranges between 10 and 20 μm, while the inside and outside diameters are 5–15 nm and 50 nm, respectively. The detailed parameters are listed in Table 1.

The matrix was composed of cement, sand, water and other additive components. P·O 42.5 cement was obtained from Guangxi Yufeng group co. Ltd. (China) and the sand from Xiamen Aisiou standard sand co. Ltd. (China). Table 2 reports on the technical properties of ordinary Portland cement. To get more compacted composite structures, silica fume was provided by Gongyi Yuanheng water purification material factory (China) with a particle size of 0.1–0.3 μm. At the same time, fly ash (Gongyi Yuanheng water purification material factory, China) was used to replace part of the cement. The related parameters of silica fume and fly ash are listed in Table 3. A defoamer (Guangdong Foshan Xushi chemical technology co. Ltd. China) was added to limit the number of bubbles produced by mixing all the components. Finally, a surfactant was used to improve the MWCNT dispersion and a water-reducing agent to improve the flexural strength of the composites. Both were obtained from the Guangdong Foshan Xushi chemical technology co. Ltd. (China).

All the formulations studied with their codes (S indicates "sample" and the number is the MWCNT weight content: 01 means 0.1% wt) are listed in Table 4. The defoamer, surfactant and water-reducing agent were kept constant at 12 ml, 12 g and 18 g, respectively. The micro-structure was analyzed using a field emission scanning electron microscope (FE-SEM) Hitachi SU-8020/X-MAX80 (Japan) at Guangxi University, China.

2.2 Sample preparation

The preparation of each specimen includes several steps. First, the standard test mold was cleaned and machine oil was applied to ensure that the slurry can fill all the mold parts. Second, each component of a composite was weighing as reported in Table 4. To avoid generating a large number of bubbles, the MWCNT solution was placed in a beaker and stirred by a digital thermostated magnetic stirrer (Jintan Dadi automation instrument factory, China) for 30 min. Third, the cement, fly ash, silica fume, water reducer and the dispersant (polyvinylpyrrolidone) were mixed together in a blender (dry-blending) for 3 min. Then, water and deformer were sequentially added and the resulting mixture was stirred for 2 min. At this time, the MWCNT was slowly added and mixing was continued for another 10 min. Fourth, the slurry was poured into the test mold having dimensions of 40 mm × 40 mm × 160 mm. Then, the test mold was placed on a vibrating table for 2 min. Finally, the test mold filled with the leveled slurry was cured at room temperature for 1 day before being demolded. Finally, all the specimens were placed in a curing room for 28 days (95% RH).

2.3 Mechanical characterization

Following the standard GB/T17671-1999, the specimen size was taken as 40 mm × 40 mm × 160 mm. Three-point bending loading mode was applied and the beam span was fixed at 100 mm. All the flexural tests were carried out according to GB/T24491-200, JGJ/T221-2019 and CECS13-2009.

To measure the strains of the specimen under flexural load, five strain gages were installed at different positions. At the mid-span of the beam, a strain gage was glued at the neutral layer, as well as the upper and the lower position which are 5 mm away from the beam surfaces. To compare the deformation at different locations, two other strain gages were glued near the hinge supports. The center of

Table 1 Physical properties of the MWCNT

Length (μm)	Inside diameter (nm)	Outside diameter (nm)	Purity (%)	Specific surface area ($m^2 \cdot g^{-1}$)	Bulk density ($g \cdot cm^{-3}$)	Density ($g \cdot cm^{-3}$)
10–20	5–15	> 50	> 98	> 60	0.18	2.1

Table 2 Technical properties of P·O 42.5 cement

Setting time (min)		Tensile strength (MPa)		Compressive strength (MPa)		MgO (%)	SO_3 (%)	Loss (%)	Cl^- (%)
Initial	Final	3 days	28 days	3 days	28 days				
≥ 45	≤ 450	≥ 4.5	≥ 7.5	≥ 22.0	≥ 44.5	≤ 4.5	≤ 3.2	≤ 5.0	≤ 0.06

the strain gage is 5 mm away from the hinge support and the bottom of the beam. Figure 1 presents a sketch of the experimental set-up with dimensions.

The static tests are composed of six groups related to the MWCNT content (Table 4) and each group contains six specimens. All the tests were carried out on a digital hydraulic testing machine (YES-300), and the strains were measured by a static strain acquisition system (JMTEST). After completion of the flexural tests, the fractured test blocks were used to test their compressive strength. From the six specimens of each group, the average compressive strength and flexural strength were obtained.

The fatigue test were divided into six groups according to the MWCNT content (Table 4). Each group includes nine specimens which were used to perform the experiment under three stress levels: 0.70, 0.75 and 0.80 of ultimate flexural load. The fatigue load can be determined by the flexural strength of MWCNT reinforced cementitious composites obtained from the static tests. Before fatigue testing, the specimens were polished via sandpaper (M40) and cleaned by alcohol (75% of ethanol). The sample dimensions and the strain gages positions are the same positions as for the static tests, and dynamic strain gages were used to collect the data. These gages were TMR 7200 from Tokyo measuring instruments laboratory co. Ltd. (Japan). The fatigue loading mode was controlled by displacement. Considering the effect of the dead load, the stress ratio was taken as 0.5. The loading applied was a sine waveform and the loading frequency was 10 Hz. The electro-hydraulic serve fatigue testing machine was HYS-100 from Changchun Hao yuan Testing Machine Co. Ltd. (China). The data were automatically obtained and analyzed by the testing system.

3 Static tests

3.1 Results

The results under static testing are reported in Table 5. It is easy to see, except the flexural strength of S03, MWCNT addition improved the mechanical strengths of the cement-based composites. The trend for both flexural and compressive strength is similar: the values increase at low MWCNT content and then decreases. The only difference is the optimum content: 0.2% for compressive strength and 0.1% for flexural strength. Nevertheless, all the values except S03 are above the neat concrete matrix value. In both cases, the increases are substantial for the low MWCNT content used: 30% and 14% for the flexural and compressive strengths, respectively.

Table 3 Physical parameters of fly ash and silica fume

Component	Density (g cm^{-3})	Bulk density ($g{\cdot}cm^{-3}$)	Specific surface area (m^2 g^{-1})	SiO_2 (%)	Al_2O_3 (%)	FeO (%)	MgO (%)	CaO (%)
Fly ash	2.1	0.78	0.33	58	30	4.3	2.8	1.5
Silica fume	1.8	0.75	15	96	1.7	1.2	0.3	0.2

Table 4 Formulation of CNT reinforced concrete studied

No	Cement (g)	Sand (g)	Fly ash (g)	Silica fume (g)	MWCNT dispersed solution (ml)	Water (g)
S00	1500	1500	150	150	0	564.0
S01	1500	1500	150	150	15	550.5
S02	1500	1500	150	150	30	537.0
S03	1500	1500	150	150	45	523.5
S04	1500	1500	150	150	60	510.0
S05	1500	1500	150	150	75	496.5

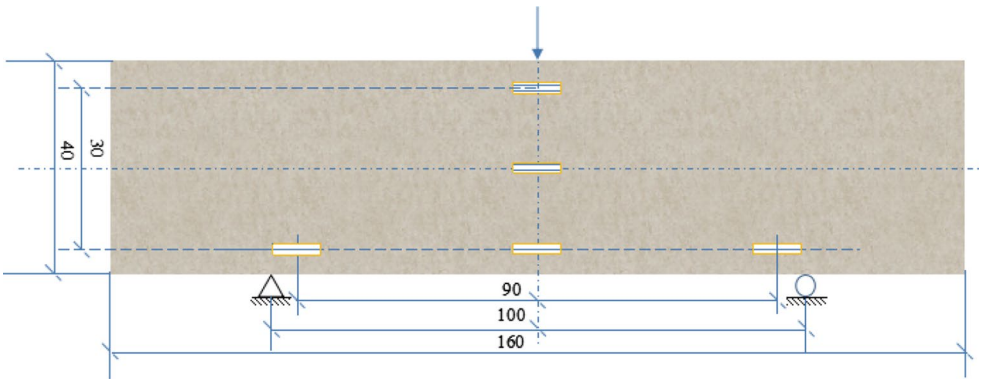

Fig. 1 Three-point bending force diagram (values are in mm)

Table 5 Static mechanical properties of MWCNT reinforced concrete

Sample	S00	S01	S02	S03	S04	S05
Compressive strength (MPa)	76.1	80.1	86.9	77.6	81.5	80.3
Flexural strength (MPa)	10.6	13.8	11.3	10.4	11.7	11.2

3.2 Comparison

Several researchers investigated the effect of MWCNT content on the compressive strength of cement-based composites. In this study, when 10% fly ash is added, the compressive strength of composites with 0.2% MWCNT increased by 14% over the plain mortar value. This is slightly higher than Chaipanich et al. [34] who reported a 8% increase when 0.5% MWCNT and 25% fly ash were added. Furthermore, Kumar et al. [33] investigated the effect of applying an ultrasonic treatment (different time) on the compressive strength of MWCNT cement composites. The compressive strength of MWCNT reinforced cement composites at 28 days was only 48.5 MPa at 0.5% MWCNT with 4 h of ultrasonic treatment which is much lower than our values (Table 6). Sikora et al. [36] added a super-plasticizer and analyzed the effects of a solid nano-silica shell on the MWCNT inside cement composites. In their case, the compressive strength of the composite was increased by 20% when 0.25% MWCNT was added. Comparing the compressive strength, the study on flexural strength of MWCNT reinforced composites is more important because of the brittleness of cement matrices. To improve MWCNT dispersion in the matrix, the mixing time of the MWCNT cementitious composites was presented by Mohsen et al. [39]. The results showed that the mixing time significantly affected the flexural strength of MWCNT cementitious composites. Furthermore, Mohsen et al. [40] suggested that a CNTs' content 0f 0.25 wt% might be an ideal content for achieving better dispersion and optimal flexural strength. Similar results were reported when the

Table 6 Formulation of the CNT reinforced concrete taken form the literature

Composition	Water/cement	References
Ordinary Portland cement (CEM I, class 42.5R), sand, water, MWCNT	0.70	Kang et al. [43]
Ordinary Portland cement (CEM I, class 42.5R), sand, water, MWCNT, surfactant (TX10)	0.55	Kang et al. [43]
Sulfur aluminates cement (42.5R), sand, water, MWCNT, dispersant	0.30	Wang et al. [42]
Ordinary Portland cement (CEM I, class 42.5R), sand, water, MWCNT, surfactant, long mixing time (60 min)	0.40	Mohsen et al. [39]
Type I 42.5R Portland cement, standard sand, water, superplasticizer, MWCNT (milled with a ball mill)	0.45	Li et al. [44]
Class G oil well cement, water, dispersant, anti-foaming agent, MWCNT	0.44	Lu et al. [45]
Portland cement (1–70 µm), fly ash (1–20 µm) or not, sand, water, MWCNT (compression)	0.50	Chaipanich et al. [34]
ASTM type 1 Portland cement, water, MWCNT, sonicated for 30 min or 4 h (compression)	0.40	Kumar et al. [33]
Ordinary Portland cement (CEM I, class 52.5R), nano-silica or not, superplasticizer, water, MWCNT (compression)	0.40	Sikora et al. [36]
Brazilian type CP-V Portland cement, water, isopropanol, MWCNT (flexion)	0.33	Rocha et al. [38]
Portland cement, CEM I, Class 42.5 R, water, fine aggregate, coarse aggregate, superplasticizer, MWCNT, mixing duration of 60 min (flexion)	0.50	Mohsen et al. [41]

MWCNT content is as low as 0.05–0.1% [38] or 0.03–0.25% [41].

To determine the effect of MWCNT content on the mechanical properties on cementitious composites, the compressive strength and flexural strength results are compared with literature data [33, 34, 36, 38–45] as plotted in Fig. 2. In general, the values of Kang et al. [43] are very low whatever a surfactant is used or not. This is probably related to their high water:cement (W:C) ratio (0.70 or 0.55 vs. 0.331–0.376 here). The results of Wang et al. [42] mainly focused on low MWCNT content (0.05% to 0.15% wt), which is similar with reference [43]. For both compressive and flexural strengths, the optimum MWCNT content is close to 0.1% wt as the values decrease at higher content, probably due to some agglomerations. To get better improvement, Mohsen et al. [39] increased their mixing time to 60 min. In this case, the compressive and flexural strengths continuously increased with MWCNT content up to 0.5% wt However, Mohsen et al. [41] showed that the specimens had lower flexural strength as the water cement ratio was taken as 0.50. When the water cement ratio is 0.45 [44] or 0.44 [45], the compressive strength and flexural strength initially increased before decreasing leading to an optimum content.

To more conveniently compare the results obtained from different references (different material compositions), a list is provided in Table 6.

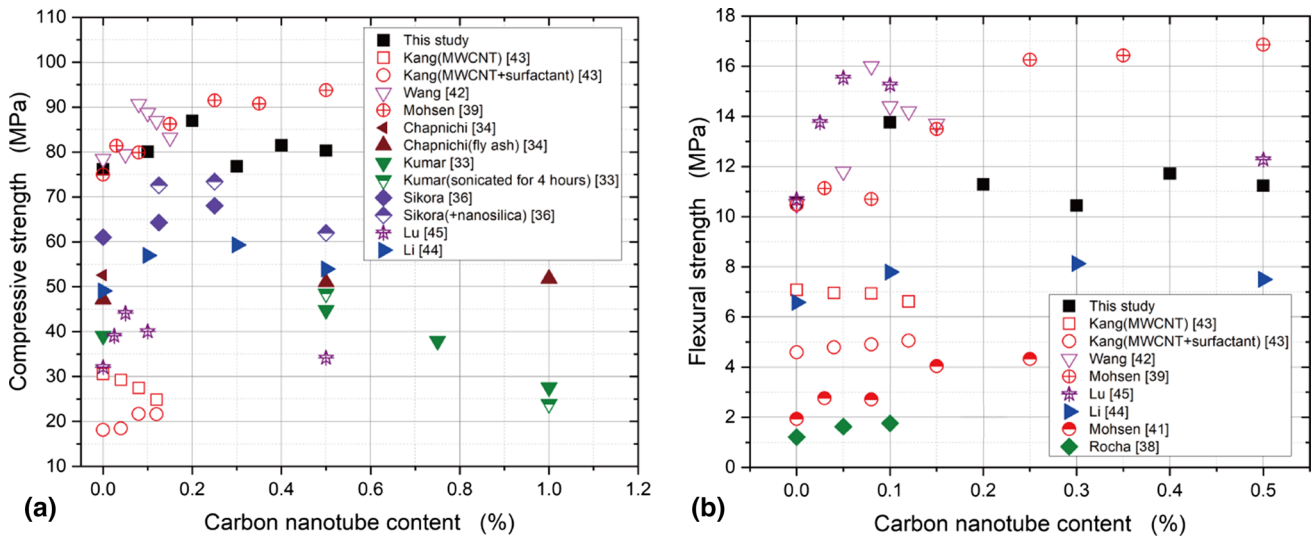

Fig. 2 Effect of MWCNT content on the mechanical properties of cement based composites. **a** Compressive strength and **b** flexural strength

4 Fatigue tests

The maximum fatigue loads under the three stress levels investigated are listed in Table 7. For all the fatigue tests, the fatigue life limit was set to 2 million cycles. If the sample can sustain 2 million cycles without breaking, the fatigue test is stopped. Again here, the strains at different locations were recorded to determine the effect of MWCNT content on the fatigue performance of cementitious composites.

In this study, HYS-100 electro-hydraulic servo fatigue testing machine and JMTEST dynamic strain connect system were selected. The scheme of the three-point flexural fatigue test set-up can be seen in Fig. 3.

4.1 Fatigue lives

The fatigue lives of MWCNT reinforced cementitious composites under three-point bending deformation are very discrete (experimental data). The reasons causing this phenomenon includes several factors such as: heterogeneity of the materials, size and quality difference, environmental conditions (temperature, humidity etc.), testing machine accuracy, loading velocity control, etc. The main reason is the dispersion of the static test results (cumulative to the fatigue test) and the sensitivity of the composites to the stress levels. Based on this information, more samples are beneficial for fatigue testing to get more accurate results. However, considering time and economic limitations, each group contained only three samples. Despite this limitation, useful results can still be obtained.

To conveniently compare the fatigue lives of cementitious composites with different MWCNT content under three stress levels, the results are plotted in Fig. 4. When the stress level increased from 0.70 to 0.75 and 0.80, the average fatigue lives of cementitious composites decreased. Although the experimental results are discrete, as the MWCNT content increases, the fatigue performance of cementitious composites can be improved. It is easy to see that the fatigue life is maximum at 0.2% MWCNT. Above 0.2%, the average fatigue lives decreased because of MWCNT agglomeration. This is especially the case at 0.3% which is associated to the lowest static flexural strength.

In general, cementitious composites fail at their mid-span. Without MWCNT, the sample show a clear brittle fracture. But when MWCNT is added, they will pull-out before breaking. This phenomenon is mainly caused by the heterogeneity of the MWCNT composites and the high MWCNT elastic

Table 7 Flexural fatigue maximum load (F_{max}) under three stress levels (kN)

Stress level	MWCNT content (%)					
	0	0.1	0.2	0.3	0.4	0.5
0.70	3.16	4.11	3.37	3.12	3.50	3.36
0.75	3.38	4.40	3.61	3.34	3.75	3.60
0.80	3.61	4.70	3.85	3.56	4.00	3.84

Stress ratio (F_{min}/F_{max}) is 0.5

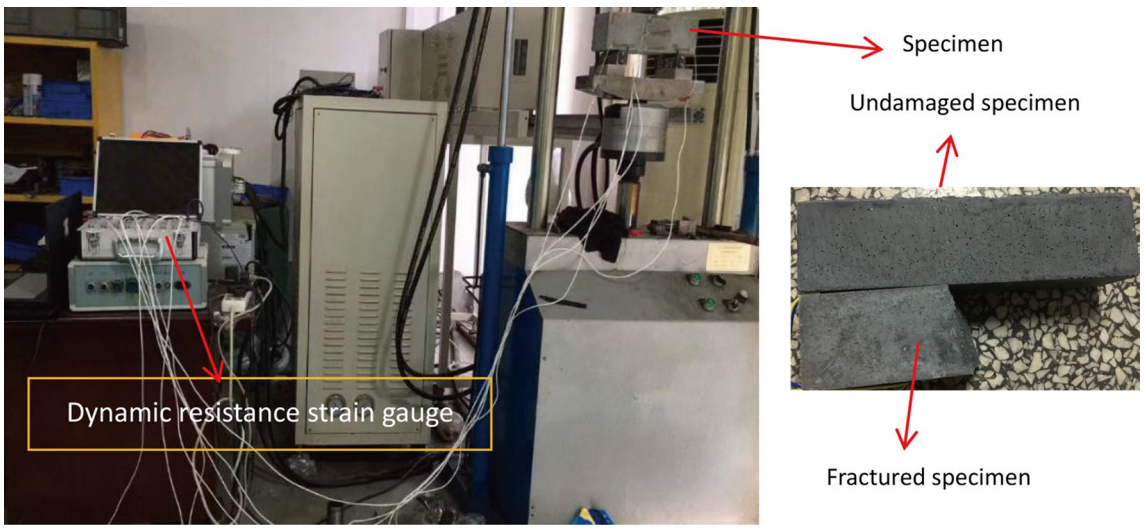

Fig. 3 Scheme of the three-point flexural fatigue test

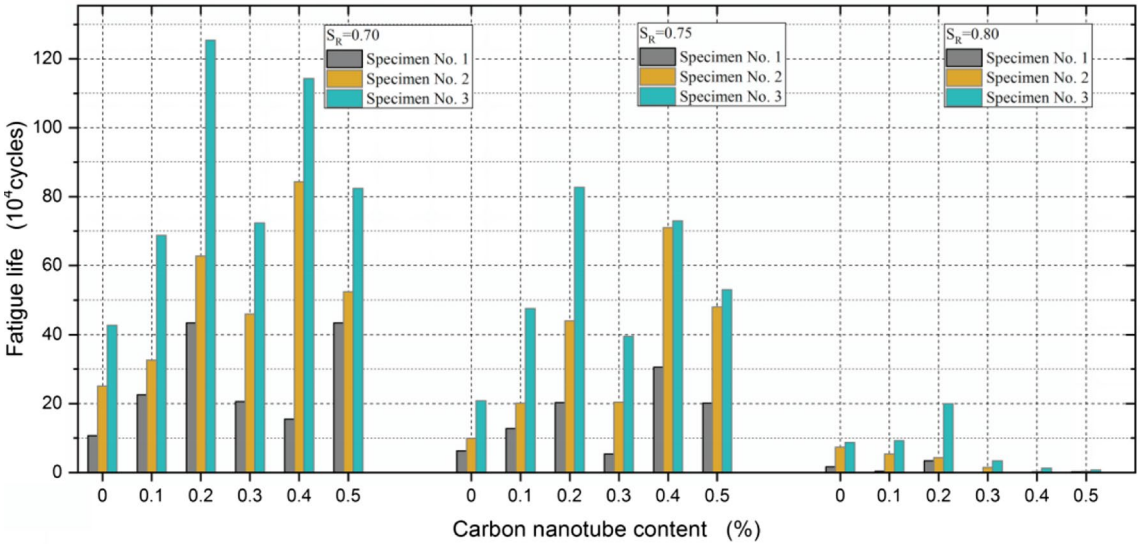

Fig. 4 Fatigue lives as a function of MWCNT content under three stress levels

modulus and tensile strength. However, it is not easy to get good MWCNT dispersion and agglomerations lead to heterogeneities (defects). For this reason, MWCNT reinforced cementitious composites sometimes fracture near the hinge support.

4.2 Strain-fatigue life curves

During the fatigue tests, the deformation of the specimen can reflect the fatigue life development of the material. Investigating the strains at different positions provides more information to analyze the fatigue behavior of the composites and better understand their damage state. Here, five strain gages were installed at different locations to get this information (Fig. 1). For the three-point bending beam, at the mid-span, the deformation of each location should be positive, negative or 0. If the size of the strain gage is ignored, the strain gages at the mid-span can measure the axial strains (tension, compression or 0). Near the beam supports, although shear deformations are present, they have a negligible effect on the strain gages measuring the tensile deformation. From the test results at mid-span, the strain of the neutral layer is close to 0 and the tensile strain at the lower location is close to the absolute value at the upper location. Similarly, the strains close to the left and right support locations are similar. To limit the amount of analysis, only the tensile strains at the mid-span and near the left support are selected to compare.

For the neat cementitious concrete, the relationships between the strain and the fatigue life are plotted in Fig. 5. The figure shows how the strains vary with the fatigue life at different positions under the stress levels studied (0.70, 0.75 and 0.80). The strains at the mid-span are higher than that near the support. It is expected that the stress level has a significant effect on the fatigue life of composites. However, it is not obvious what is the relation between the strain at different positions and this is what needs to be determined.

All the strain–fatigue life curves include three stages: initial increase followed by a stable stage (plateau) and finally a rapid increase. In the stable stage, the strains slowly increase with the number of cyclic load and the curve is close to a straight line. In general, it is obvious that the strain reaches a maximum when the beam fractures. However, the last strain value near the support is not the maximum of this material, which is different than the value at mid-span. If MWCNT are added into the matrix, similar results are observed. When the MWCNT content is 0.1%, the relationship between the strain and the fatigue life at two positions under the three stress levels is plotted in Fig. 6. In this case, the curves are composed of three stages like for the neat concrete and a similar behavior was observed for all the other MWCNT contents.

To further understand the three stages and the relation between the axial strain and the fatigue life, both parameters were normalized for the three stress levels. When the stress level is 0.70, the normalized axial strain—normalized fatigue life curves at different locations are plotted in Fig. 7a and b. It can be seen that the axial strain rapidly increases in the first stage as MWCNT is added. When the stress level is taken as 0.75, the results are similar (Fig. 7c and d), especially the axial strain increasing in the first stage is obvious for 0.3% MWCNT. However, if the stress level is increased to 0.8, the MWCNT have no significant effect on the axial strain developing in the first stage (Fig. 7e and f). These results indicate that under lower stress level, in the stable second stage, MWCNT reinforced cement-based composites

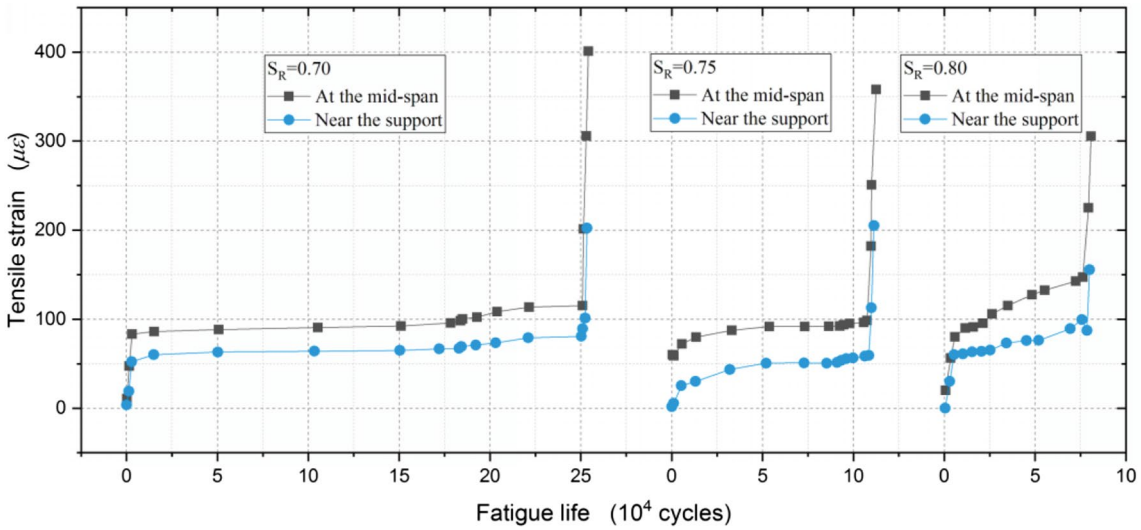

Fig. 5 Tensile strength—fatigue life curves without MWCNT under a stress level of 0.70, 0.75 and 0.8

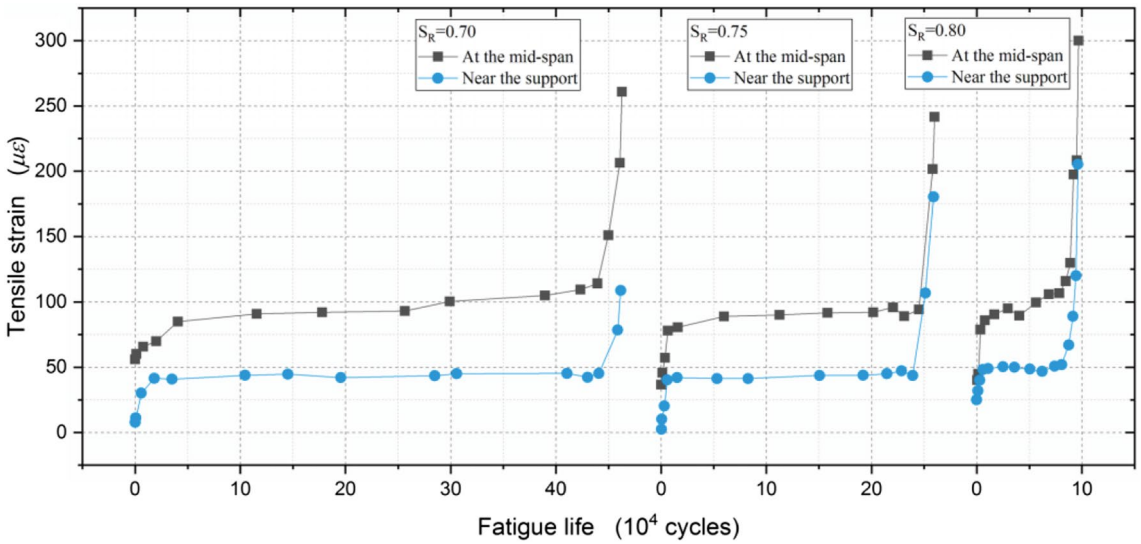

Fig. 6 Tensile strength—fatigue life curves at 0.1% MWCNT under a stress level of 0.70, 0.75 and 0.8

have higher axial strain and can absorb more energy before failure, which is very interesting to investigate further.

4.3 Fatigue curves

(1) S–N curves

In terms of fatigue test data and static strength (cycle number = 0), linear regression analysis was used to determine the relationships between the stress level (0.70, 0.75, 0.80, and 1.00) and the logarithm of the fatigue lives. The results are plotted in Fig. 8a and the fitting parameters are reported in Table 8. From this figure, the cycle number is 1 when the stress level is taken as unity. Although all the curves are close to each other, the fitting curves trends are obvious. The fatigue life increases with MWCNT content up to 0.2% (solid lines), while the fatigue life decreases due to MWCNT agglomeration (dashed lines) above 0.2%. For all cases, the coefficients of determination are higher than 0.85 indicating that the stress level is linearly related to the log of fatigue life.

Another way to analyze the fatigue properties of materials is via a standard stress level (S)-number of cycle to failure (N) curve [46]. Based on this relationship, several models have been proposed to predict the data: power-law,

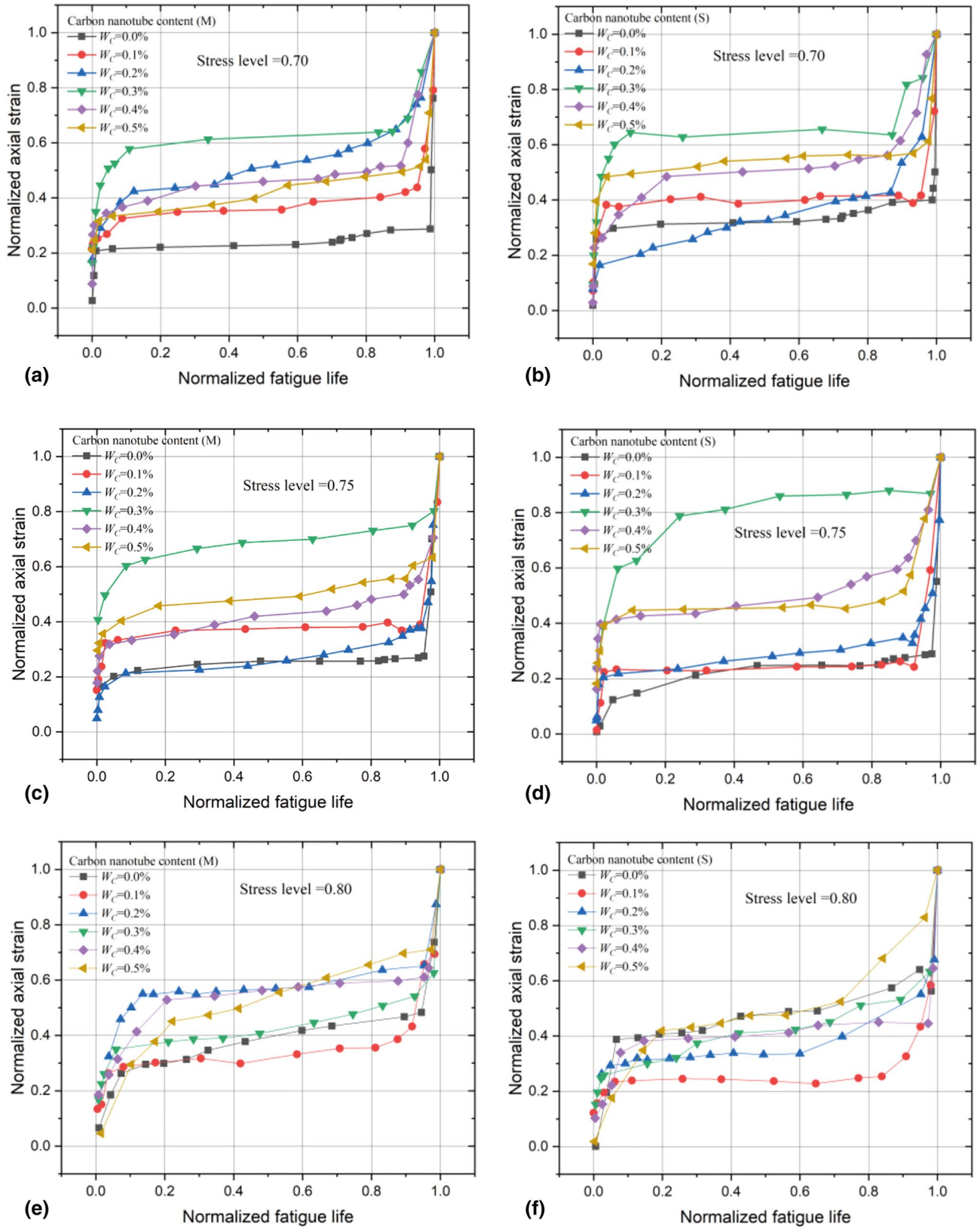

Fig. 7 Normalized strain—normalized fatigue life curves under different stress levels: **a**, **c**, **e** at midspan **b**, **d**, **f** near the support

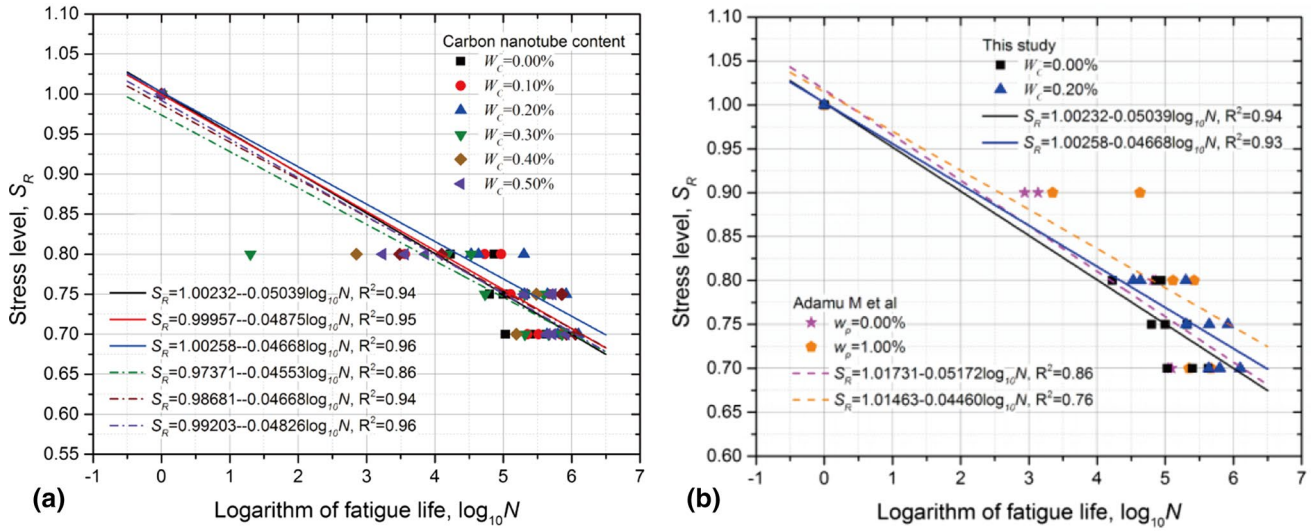

Fig. 8 Stress level—fatigue life curves. **a** Effect of MWCNT content and **b** comparison with Adamu et al. [47]

Table 8 Fitting parameters for Eq. (2)

Parameters	Nanoparticle content (%)							
	0.0	0.1	0.2	0.3	0.4	0.5	0 [47]	1 [47]
n_p	12	12	12	12	12	12	8	8
n_d	10	10	10	10	10	10	6	6
RSS	0.0082	0.0069	0.0059	0.0192	0.0092	0.0050	0.0121	0.0206
a								
Value	1.0023	0.9996	1.0026	0.9737	0.9868	0.9920	1.0173	1.0146
δ	0.0163	0.0149	0.0138	0.0229	0.0163	0.0122	0.0299	0.0400
b								
Value	− 0.0504	− 0.0488	− 0.0467	− 0.0455	− 0.0467	− 0.0483	− 0.0517	− 0.0446
δ	0.0038	0.0033	0.0029	0.0054	0.0037	0.0028	0.0078	0.0093
R^2	0.9476	0.9555	0.9621	0.8767	0.9411	0.9678	0.8793	0.7943
Adj. R^2	0.9424	0.9511	0.9583	0.8644	0.9353	0.9645	0.8592	0.7600
Pearson's r	− 0.9735	− 0.9775	− 0.9809	− 0.9363	− 0.9701	− 0.9838	− 0.9377	− 0.8912

n_p is the number of points, n_d is the degree of freedom, *RSS* is the residual sum of square, δ is the standard error, R^2 is the coefficient of determination

exponential and three parameters series. Here, a logarithmic relation (similar to a power-law) is proposed as:

$$S_R = a + b \log_{10} N \tag{1}$$

where a and b are fitting parameters.

To further understand the fatigue life curves of MWCNT reinforced cementitious composites, the fitting curves in Fig. 8b are compared with literature results. From the fitting curves, the fatigue life of our composites are slightly compared to the results of Adamu et al. [47]. However, our MWCNT content (0.1–0.5%) is much lower than their nano-silica content (0.0–1.0%) and the coefficient of determination is also higher. Also, their water:cement ratio is 0.36 which is close to our value (0.331–0.376%). For example, if the stress level is 0.70, the average fatigue lives of roller compacted concrete are 116,821, 167,079, and 345,879 for samples without nano-silica fume and crumb rubber, with rubber crumb alone or with both nano-silica fume and crumb rubber. This indicates that adding 1% wt of nano-silica fume increased the fatigue life by 196% and 107% to the two former. In this study, the average fatigue lives are 261,780 and 771,848 which indicates that the fatigue life was increased by 195% by adding 0.2% MWCNT. This clearly shows that MWCNT is much better than nano-silica to improve the fatigue life of cementitious materials.

To better compare the results between both cases, all the fitting parameters are listed in Table 8. It can be seen that the

coefficient of determination is very close to the correlation coefficient and always higher than 0.85. On the other hand, the coefficient of determination is only 0.76 when the nano-silica content is 1.0% for reference [47]. It is worth noting that the static flexural strength is accounted for in the linear regressions, so the number points for each fitting curve is 2.

4.4 Optimal MWCNT content

To better see the effect of MWCNT content on the fatigue life of cement-based composites, the average fatigue life of each group of sample is plotted in Fig. 9a. It can be seen that the optimal MWCNT content is 0.2%. Although there might be some differences between loading type, this result is in agreement with the static compressive tests (Table 5). Figure 9a shows that the fatigue lives are decreasing above 0.2% MWCNT. So a bi-linear model was proposed to represent all the data as plotted in Fig. 9b:

$$\begin{aligned} N &= C_1 + D_1 w_c \quad w_c < 0.2\% \\ N &= C_2 + D_2 w_c \quad w_c \geq 0.2\% \end{aligned} \tag{2}$$

where C_1, C_2, D_1 and D_2 are regression coefficients. With the fitting parameters listed in Table 9, a good correlation between the fatigue life and the MWCNT content is obtained with coefficients of correlation above 0.80. For this linear regression, to get better fitting, the intercept or the slope were separately fixed. This is why no standard error (−) is reported in Table 9.

5 Micro-mechanism analyses

Figure 10a–d presents the fracture cross-sections of the specimens for 0%, 0.2%, 0.3% and 0.5% MWCNT, respectively. Figure 10a shows that the specimen is relatively dense without significant porosity. When MWCNT are added, because of their higher elastic modulus and tensile strength, the mechanical properties of the composites are improved. However, Fig. 10b shows that the presence of MWCNT produced some porosity (in red rectangle) in the specimen, which increased with their content. This morphological change can lead to lower mechanical performances (static and fatigue) of the composites depending on the composition. This is especially the case above 0.2% MWCNT, it is clearly seen in Fig. 10c and d that more pores result in corresponding mechanical properties decreasing. In both images, MWCNT agglomeration is observed resulting in a higher number of larger defects (in red rectangles) leading to lower mechanical properties.

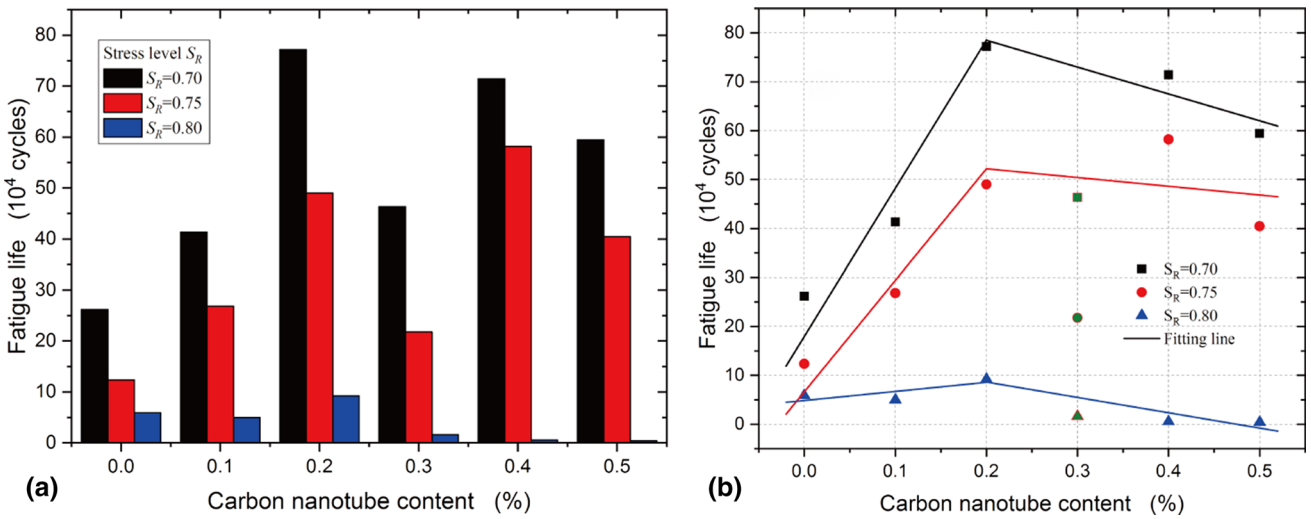

Fig. 9 Relationship between the average fatigue life and MWCNT content. **a** Column diagram and **b** bi-linear regression analyses

Table 9 Regression parameters for Eq. (2)

Stress level	C_1		D_1		C_2		D_2		Adj. R^2
	value	δ	value	δ	value	δ	value	δ	
0.70	17.9405	4.4211	302.9	–	89.4652	1.9820	− 54.9000	–	0.8855
0.75	6.6104	2.8798	227.9	–	55.7810	–	− 17.9038	12.5991	0.9491
0.80	4.8598	–	17.7874	6.7022	14.9142	0.9215	− 31.4000	–	0.9270

δ is standard error

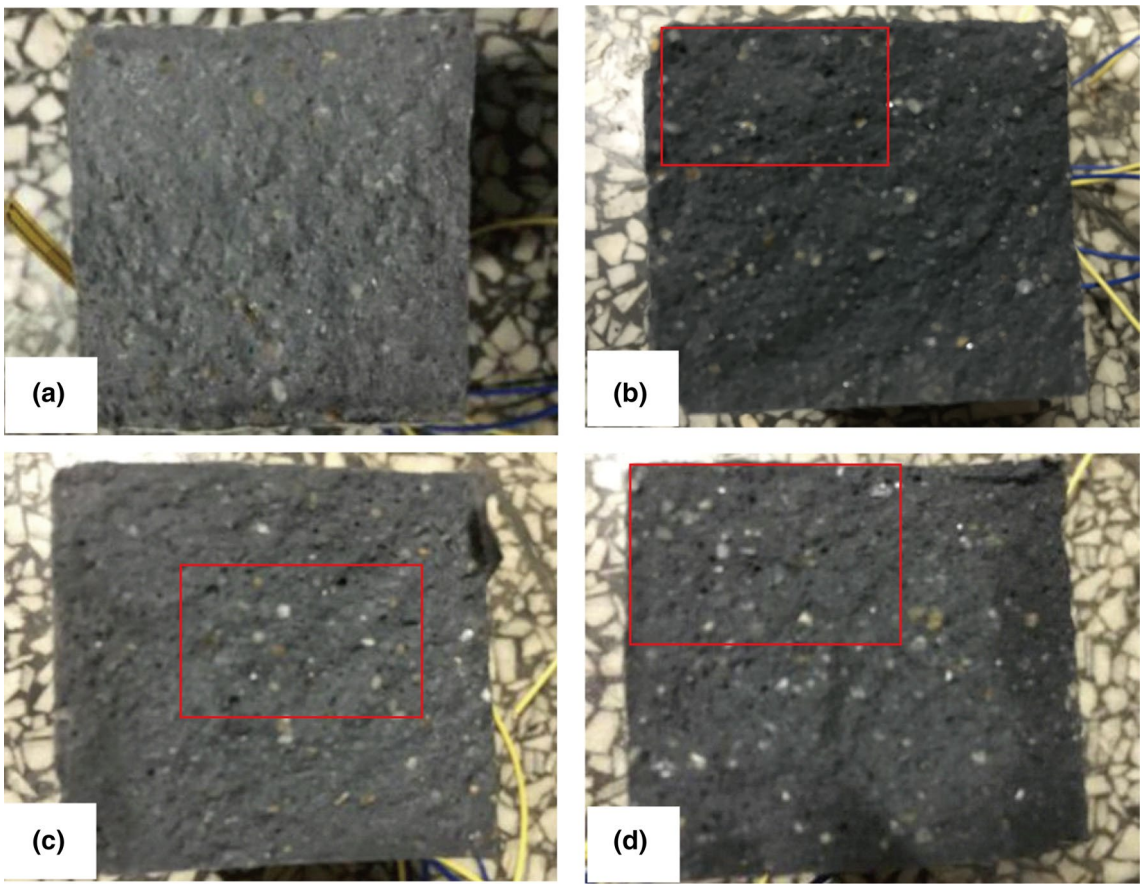

Fig. 10 Cross-section of specimens after failure. **a** Pure mortar, **b** cementitious with 0.2% MWCNT, **c** cementitious with 0.3% MWCNT and **d** cementitious with 0.5% MWCNT

To ensure a good bonding between the cement matrix and MWCNT, during the mixing of several components, polyvinylpyrrolidone was added into the matrix as a binder. Scanning electron microscopy (SEM) can be used to analyze the microscopic enhancement mechanism of MWCNT. Figure 11a presents an image of the MWCNT. Figure 11b presents a micro-topography of the concrete without MWCNT. It can be seen that the micro-structure of the specimen is loose. A large number of hydrated crystals and several micro-pores are observed which can decrease the mechanical properties of the composites. The microstructural analysis also shows the ability of some MWCNT to bridge cracks forming strands at the micron scale. These strands are cement products other than MWCNT showing crack bridging at different positions which are improving the matrix properties.

The microstructural investigation also shows several locations without MWCNT indicating that they were covered by calcium-silicate-hydrate (C–S–H) products or not properly dispersed in the cement matrix (not uniform distribution). On the other hand, some MWCNT can be imbedded within the cement compound products or penetrate the C–S–H crystals' surface (Fig. 11c) to play a bridging role in the matrix and improve the mechanical performance of the composites. Owing to their very high length/diameter ratio, MWCNT can easily entangle in the cement matrix, especially when the weight fraction increases above 0.2% in our case (optimal content). To better discriminate the MWCNT from the matrix, higher magnification was used and Fig. 11d shows clear MWCNT agglomeration in the matrix.

Nevertheless, the SEM images of Fig. 11 show that the MWCNT are well embedded in the cement paste. Despite being teared and pulled-out, the interface between the MWCNT and the matrix is not broken. This means that MWCNT and cement paste have good interfacial adhesion. Inside the composites, the MWCNT are connected with cement or other MWCNT to form a regular network which can better resist a higher level of external load. However, the MWCNT tend to clump and entangle together when they are dispersed in the matrix, especially if the MWCNT content is higher (0.2% here). This phenomenon seems to be more important on decreasing the fatigue life than the static properties. Nevertheless, more work is needed to better

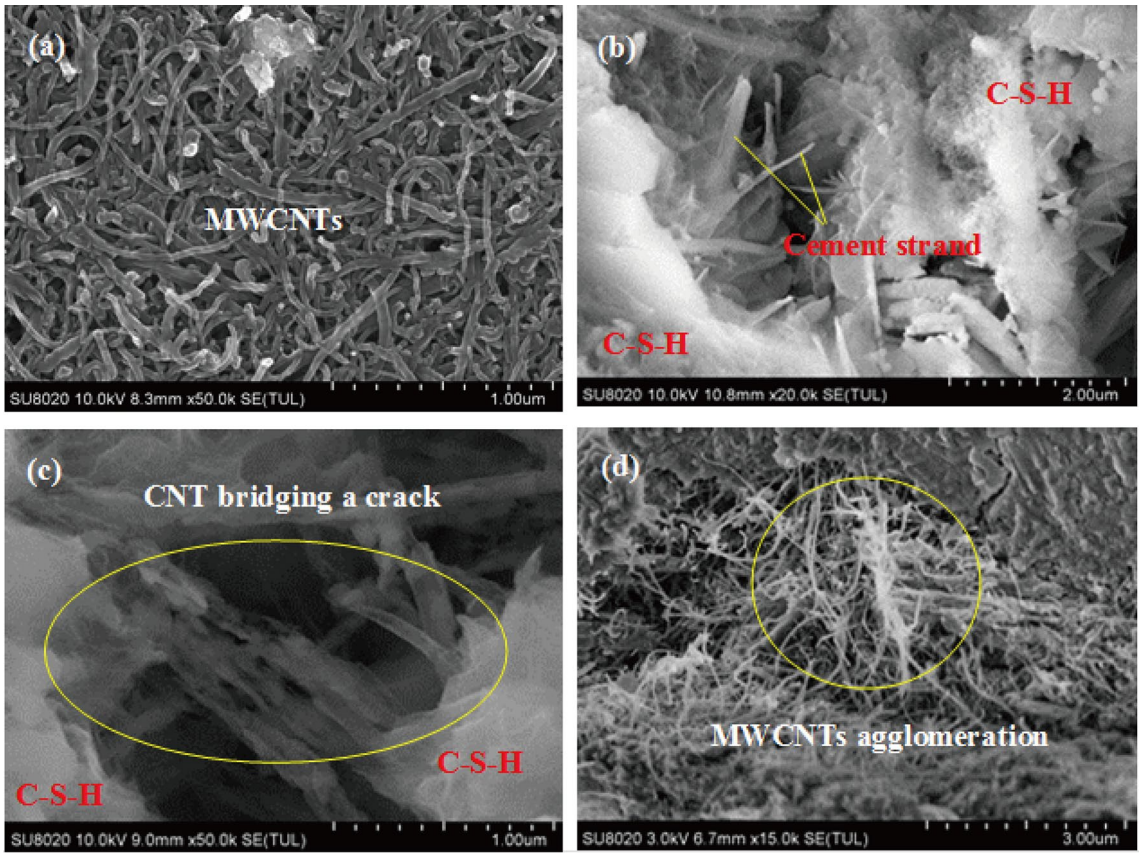

Fig. 11 SEM image of **a** MWCNT; **b** composite without MWCNT; **c** cementitious composite with low MWCNT content and **d** cementitious composite with high MWCNT content

understand the structure-properties relations for these complex materials.

6 Conclusions

As a high strength and high stiffness nano-material, WMCNT were added into a cement matrix to modify the mechanical (flexural) performance under both static and cyclic loading. From both types of tests, the flexural strength and fatigue life of these nano-composites were investigated for a MWCNT content between 0.1 and 0.5% wt. At the same time, the micro-mechanism of MWCNT improving the mechanical properties was also discussed. Based on the results obtained, regression models were proposed and compared with literature data. The main results are listed as follows:

1. From the static tests, the optimal MWCNT content to improve the compressive strength and flexural strength of cement-based composites was found to be 0.2% and 0.1%, respectively. Compared with data taken from the literature, it was shown that the water:cement ratio has a significant effect on the strength of MWCNT cement-based composites. On the other hand, silica fume and increased mixing time both led to MWCNT deagglomeration in the cement matrix leading to improved composites strength.
2. The fatigue results revealed that the optimal MWCNT content to improve the fatigue life of the composites was 0.2%. A bi-linear regression analysis was performed for each stress level ($S_R = 0.7$, 0.75 and 0.8) which highly corelated the fatigue life (N) of the composites for the range of MWCNT content studied. Compared with literature data using nano-silica in a cement matrix, our results seem to be better due to a much lower nano-particles content used (0.2% vs. 1%).
3. SEM analyses revealed that good interfacial adhesion between the MWCNT and the cement matrix was obtained, which improved the mechanical performance at low content via a bridging effect. However, the hollow and thin wall micro-structure of MWCNT is easy to bend and its large surface area led to agglomeration creating defects (weak points) in the matrix. As a result, lower mechanical performances of the composites was observed at higher (above 0.2%) MWCNT con-

centration. Nevertheless, this optimum content can be improved in future work to achieve the maximum potential reinforcement of MWCNT.

Acknowledgements This study was supported by Zhejiang Provincial Natural Science Foundation of China (Grant number: LY18E080028), National Natural Science Foundation of China (Grant number: 51568009) and Wenzhou Science and Technology Project, China (Grant number: S20190001).

Declarations

Conflict of interest We declare that we do not have any commercial or associative interest that represents a conflict of interest in connection with the work submitted.

Ethical approval This article does not contain any studies with human participants or animals performed by any of the authors.

References

1. Lee MK, Barr BIG. An overview of the fatigue behaviour of plain and fibre reinforced concrete. Cement Concr Comp. 2004;26(4):299–305.
2. Choi SJ, Mun JS, Yang KH, Kim SJ. Compressive fatigue performance of fiber-reinforced lightweight concrete with high-volume supplementary cementitious materials. Cement Concr Comp. 2016;73:89–97.
3. Medeiros A, Zhang XX, Ruiz G, Yu RC, Velasco MDL. Effect of the loading frequency on the compressive fatigue behavior of plain and fiber reinforced concrete. Int J Fatigue. 2015;70:342–50.
4. Silva FD, Mobasher B, Toledo RD. Fatigue behavior of sisal fiber reinforced cement composites. Mater Sci Eng A Struct. 2010;527(21–22):5507–13.
5. Makita T, Bruhwiler E. Tensile fatigue behaviour of ultra-high performance fibre reinforced concrete (UHPFRC). Mater Struct. 2014;47(3):475–91.
6. Isojeh B, El-Zeghayar M, Vecchio FJ. Fatigue behavior of steel fiber concrete in direct tension. J Mater Civil Eng. 2017;29(9):04017130.
7. Deng ZC. The fracture and fatigue performance in flexure of carbon fiber reinforced concrete. Cement Concr Comp. 2005;27(1):131–40.
8. Zhang HL, Tian KL. Properties and mechanism on flexural fatigue of polypropylene fiber reinforced concrete containing slag. J Wuhan Univ Technol. 2011;26(3):533–40.
9. Yu TL, Li CY, Lei JQ, Zhang HX. Fatigue of concrete beams strengthened with glass-fiber composite under flexure. J Compos Constr. 2011;15(4):557–64.
10. Banjara NK, Ramanjaneyulu K, Sasmal S, Srinivas V. Flexural fatigue performance of plain and fibre reinforced concrete. Trans Indian Inst Metals. 2016;69(2):373–7.
11. Chen M, Zhong H, Zhang MZ. Flexural fatigue behaviour of recycled tyre polymer fibre reinforced concrete. Cement Concr Comp. 2020;105:103441.
12. Wang W, Wu SG, Dai HZ. Fatigue behavior and life prediction of carbon fiber reinforced concrete under cyclic flexural loading. Mater Sci Eng A Struct. 2006;434(1–2):347–51.
13. Mohamadi MR, Mohandesi JA, Homayonifar M. Fatigue behavior of polypropylene fiber reinforced concrete under constant and variable amplitude loading. J Compos Mater. 2013;47(26):3331–42.
14. Carless DM, de la Fuente A, Cavalaro SHP. Fatigue of cracked high performance fiber reinforced concrete subjected to bending. Constr Build Mater. 2019;220:444–55.
15. Parvez A, Foster SJ. Fatigue behavior of steel-fiber-reinforced concrete beams. J Struct Eng. 2015;141(4):04014117.
16. Saoudi N, Bezzazi B. Flexural fatigue failure of concrete reinforced with smooth and mixing hooked-end steel fibers. Cogent Eng. 2019;6(1):1594508.
17. Graeff AG, Pilakoutas K, Neocleous K, Peres MVNN. Fatigue resistance and cracking mechanism of concrete pavements reinforced with recycled steel fibres recovered from post-consumer tyres. Eng Struct. 2012;45:385–95.
18. Smrkic MF, Damjanovic D, Baricevic A. Application of recycled steel fibres in concrete elements subjected to fatigue loading. Gradevinar. 2017;69(10):893–905.
19. Alsaif A, Garcia R, Figueiredo FP, Neocleous K, Christofe A, Guadagnini M, Pilakoutas K. Fatigue performance of flexible steel fibre reinforced rubberised concrete pavements. Eng Struct. 2019;193:170–83.
20. Al-Azzawi BS, Karihaloo BL. Flexural fatigue behavior of a self-compacting ultrahigh performance fiber-reinforced concrete. J Mater Civil Eng. 2017;29(11):04017210.
21. Murali G. Statistical scrutinize of flexural fatigue strength of self-compacting steel fibre reinforced concrete beams. J Appl Sci Eng. 2018;21(2):155–62.
22. Goel S, Singh SP, Singh P. Flexural fatigue strength and failure probability of self compacting fibre reinforced concrete beams. Eng Struct. 2012;40:131–40.
23. Goel S, Singh SP. Fatigue performance of plain and steel fibre reinforced self compacting concrete using *S–N* relationship. Eng Struct. 2014;74:65–73.
24. Germano F, Tiberti G, Plizzari G. Post-peak fatigue performance of steel fiber reinforced concrete under flexure. Mater Struct. 2016;49(10):4229–45.
25. Stephen SJ, Gettu R. Fatigue fracture of fibre reinforced concrete in flexure. Mater Struct. 2020;53(3):53–6.
26. Kaur G, Singh SP, Kaushik SK. Influence of mineral additions on flexural fatigue performance of steel fibre reinforced concrete. Mater Struct. 2016;49(10):4101–11.
27. Rios JD, Cifuentes H, Yu RC, Ruiz G. Probabilistic flexural fatigue in plain and fiber-reinforced concrete. Materials. 2017. https://doi.org/10.3390/ma10070767.
28. Banjara NK, Ramanjaneyulu K. Experimental investigations and numerical simulations on the flexural fatigue behavior of plain and fiber-reinforced concrete. J Mater Civil Eng. 2018;30(8):04018151.
29. Mulheron M, Kevern JT, Rupnow TD. Laboratory fatigue and toughness evaluation of fiber-reinforced concrete. Transp Res Rec. 2015;2508:39–47.
30. Huang BT, Li QH, Xu SL. Fatigue deformation model of plain and fiber-reinforced concrete based on Weibull function. J Struct Eng. 2019;145(1):04018234.
31. Bawa S, Singh SP. Fatigue performance of self-compacting concrete containing hybrid steel-polypropylene fibres. Innov Infrastruct Solut. 2019;4(1):4–57.
32. Sobolkina A, Mechtcherine V, Khavrus V, Maier D, Mende M, Ritschel M, Leonhardt A. Dispersion of carbon nanotubes and its influence on the mechanical properties of the cement matrix. Cement Concr Comp. 2012;34(10):1104–13.
33. Kumar S, Kolay P, Malla S, Mishra S. Effect of multiwalled carbon nanotubes on mechanical strength of cement paste. J Mater Civil Eng. 2012;24(1):84–91.

34. Chaipanich A, Nochaiya T, Wongkeo W, Torkittikul P. Compressive strength and microstructure of carbon nanotubes-fly ash cement composites. Mat Sci Eng A Struct. 2010;527(4–5):1063–7.
35. Kim HK, Nam IW, Lee HK. Enhanced effect of carbon nanotube on mechanical and electrical properties of cement composites by incorporation of silica fume. Compos Struct. 2014;107:60–9.
36. Sikora P, Elrahman MA, Chung SY, Cendrowski K, Mijowska E, Stephan D. Mechanical and microstructural properties of cement pastes containing carbon nanotubes and carbon nanotube-silica core-shell structures, exposed to elevated temperature. Cement Concr Comp. 2019;95:193–204.
37. Irshidat MR, Al-Saleh MH. Flexural strength recovery of heat-damaged RC beams using carbon nanotubes modified CFRP. Constr Build Mater. 2017;145:474–82.
38. Rocha VV, Ludvig P, Trindade ACC, Silva FD. The influence of carbon nanotubes on the fracture energy, flexural and tensile behavior of cement based composites. Constr Build Mater. 2019;209:1–8.
39. Mohsen MO, Al-Nuaimi N, Al-Rub RKA, Senouci A, Bani-Hani KA. Effect of mixing duration on flexural strength of multi walled carbon nanotubes cementitious composites. Constr Build Mater. 2016;126:586–98.
40. Mohsen MO, Taha R, Taqa AA, Shaat A. Optimum carbon nanotubes' content for improving flexural and compressive strength of cement paste. Constr Build Mater. 2017;150:395–403.
41. Mohsen MO, Al-Ansari MS, Taha R, Al-Nuaimi N, Taqa AA. Carbon nanotube effect on the ductility flexural strength, and permeability of concrete. J Nanomater. 2019;2019:1–11.
42. Wang B, Xing Y, Li J. Mechanical properties and microstructure of sulfur aluminate cement composites reinforced by multi-walled carbon nanotubes. J Wuhan Univ Technol Mater Sci Ed. 2018;33(1):102–7.
43. Kang J, Al-Sabah S, Theo R. Effect of single-walled carbon nanotubes on strength properties of cement composites. Materials (Basel). 2020. https://doi.org/10.3390/ma13061305.
44. Li WW, Ji WM, Wang YC, Liu Y, Shen RX, Xing F. Investigation on the mechanical properties of a cement-based material containing carbon nanotube under drying and freeze-thaw conditions. Materials. 2015;8(12):8780–92.
45. Lu SC, Wang XY, Meng ZR, Deng QC, Peng FF, Yu CC, Hu X, Zhao Y, Ke YC, Qi FZ. The mechanical properties, microstructures and mechanism of carbon nanotube-reinforced oil well cement-based nanocomposites. RSC Adv. 2019;9(46):26691–702.
46. Schijve J. Fatigue of structures and materials. Dordrecht: Kluwer Academic; 2001.
47. Adamu M, Mohammed BS, Shafiq N, Liew MS, Zampieri P. Effect of crumb rubber and nano silica on the fatigue performance of roller compacted concrete pavement. Cogent Eng. 2018;5(1):1436027.